FROM STEADY-STATE TO TRANSIENT: IMPLICATIONS OF SUBHOURLY TEMPERATURE MODELLING IN PVSYST

Auriane Canesse, Luca Antognini, André Mermoud, Michele Oliosi, Robin Vincent, Bruno Wittmer
PVsyst SA,
Route de la Maison-Carrée 30,
1242 Satigny, Switzerland

ABSTRACT: PVsyst version 8.1 introduces subhourly simulation capabilities, which require the adoption of a transient photovoltaic (PV) module temperature model to capture the thermal inertia of PV modules. We present the PVsyst transient temperature model, an adaptation of Prilliman's exponentially weighted moving average model, and validate it analytically and against published 1-minute measurements from an open-field and a rooftop PV array. The model's impact on simulated energy yield is analysed by comparing the existing steady-state temperature model to its transient extension, with particular attention to the dependence on model parameter choice and simulation time step duration. The transient model is shown to reduce the module temperature RMSE by about 2 °C, leading to an RMSE reduction of up to 0.9 % on the simulated DC yield.
Keywords: PVsyst, validation, module temperature, transient model

1 INTRODUCTION

Subhourly PV system simulations are required to improve the precision and accuracy of energy yield calculations. This is motivated, for example, by the rapid variation of irradiance on cloudy days, which can result in more frequent occurrences, at finer timescales, of PV production exceeding the inverter clipping threshold [1]. However, certain steps of the modelling chain necessitate adaptations to correctly represent the PV system at shorter time scales. In particular, the thermal behaviour of a PV module shows a non-negligible inertia in response to these rapid environmental changes, with timescales in the range of 4–16 min for utility-scale systems [2] and potentially slower for BIPV configurations. A popular and simple approach among PV simulation software packages is given by Prilliman's method [3]. It transforms established models for steady-state PV module temperature into transient ones by applying an exponentially weighted moving average over preceding time steps. It has been shown to consistently reduce the RMSE of the temperature prediction of several steady-state models when describing subhourly data [4]. However, its original formulation and validation were limited to a specific configuration that was simulated with finite element method, consisting of a single fixed-tilt module. This therefore calls for a wider validation against experimental data from different PV system types.

This article describes an extension to the Prilliman model and evaluates its reliability when applied to a broader range of PV system configurations and to conditions of uncertain wind measurement. Section 2 presents the PVsyst transient model as an adaptation of Prilliman's formulation, together with its analytical validation against the 1D heat equation. Both steady-state and transient temperature models are then validated against measurements from two PV installations of the NIST campus, an open-field and a rooftop array [5]. Section 3 compares the modelled module temperature to 1-minute measurements and quantifies the expected impact on the simulated DC yield; Section 4 compares the simulated DC yield to the measured production and examines the influence of the simulation time step duration.

2 PVSYST PV TEMPERATURE MODEL

Computing the derating due to the PV cells operating temperature (−0.2 to −0.4 %/°C) is an important step in the PVsyst modelling pipeline. The computation is done in two steps: first, an energy balance model is used to compute the steady-state temperature at all simulation steps. An exponentially weighted moving average is then applied to obtain a realistic transient temperature.

2.1 Steady-state temperature model

The PVsyst steady-state temperature model is a thermal balance model based on plane-of-array irradiance G, ambient temperature T_{amb}, wind speed W_s, module efficiency η and module absorptance α,

$$T_{SS} = T_{amb} + \frac{\alpha\, G(1-\eta)}{U_c + U_v W_s}, \qquad (1)$$

where the heat transfer coefficients U_c (constant term) and U_v (wind dependence) are effective parameters, specific to each system. In absence of local wind measurement, W_s is set to zero and a single U coefficient is used. For hourly simulations, this model alone accurately predicts the mean module temperature, assumed to be the cell temperature. However, for minute-scale simulations, steady-state conditions do not hold anymore, and module thermal inertia must be taken into account.

2.2 Transient temperature model

A steady-state thermal model can be transformed into a transient thermal model by applying an exponentially weighted moving average over preceding time steps, as demonstrated by Prilliman [3]. The transient temperature from Prilliman's model is given by

$$T_{\mathrm{Prill,i}} = \frac{\sum_{k=i-1}^{(t_i-t_{i-1})\le(t_i-t_k)\le\Delta t_c} T_{\mathrm{SS,k}} e^{-P_k(t_i-t_k)}}{\sum_{k=i-1}^{(t_i-t_{i-1})\le(t_i-t_k)\le\Delta t_c} e^{-P_k(t_i-t_k)}}, \qquad (2)$$

where Δt_c is the cut-off time and $P_k = 1/\tau$ is the inverse of the relaxation time, computed at each time step from a set of four coefficients and depending on wind speed and module unit mass m_u in kg/m^2, defined as:

10.4229/EUPVSEC2026/4CV.1.3
020296-001

$$P_k = 0.0046 + 0.00046W_{s,k} - 0.00023m_u - 0.000016W_{s,k}m_u. \quad (3)$$

Note how equation (2) does not consider the present time step at time t_i. Several adaptations were made to the original model:

- The cut-off time was increased from 20 minutes to $\Delta t_c = 3 \times \tau_{max}$, where τ_{max} is the maximum relaxation time at zero wind speed.
- An additional averaging step was added so that the temperature T_i represents the average temperature of the time interval $[t_i, t_{i+1}[$, as is the PVsyst convention.

The transient temperature at time t in the interval $[t_i, t_{i+1}[$ is defined as

$$T(t) = \left(T_{\text{Prill,i+1}} - T_{\text{Prill,i}}\right)(1 - e^{-P_i t}) + T_{\text{Prill,i}} \quad (4)$$

The average transient temperature over the interval $[t_i, t_{i+1}[$ of duration $\Delta t = t_{i+1} - t_i$ can then be calculated analytically by

$$T_i \equiv \langle T(t)\rangle_i = \frac{1}{\Delta t}\int_{t_i}^{t_{i+1}} T(t')\mathrm{d}t' = \left(T_{Prill,i+1} - T_{Prill,i}\right)\left[1 + \frac{e^{-P_i \Delta t} - 1}{P_i \Delta t}\right] + T_{Prill,i}\,. \quad (5)$$

2.3 Analytical validation

These modifications to the Prilliman model have been validated analytically using the 1D heat equation for a thin object,

$$\frac{dT_{\text{trans}}(t)}{dt} = \frac{T_{\text{ss}}(t) - T_{\text{trans}}(t)}{\tau}, \quad (6)$$

where $\frac{d^2T}{dx^2}$ was neglected, $T_{\text{trans}}(t)$ is the instantaneous module temperature, $T_{\text{ss}}(t)$ is the steady-state temperature toward which the transient temperature converges after infinite time if the conditions were kept constant, and τ is the thermal relaxation time. The general solution to this differential equation is

$$T_{\text{trans}}(t) = e^{-t/\tau}\left[C + \frac{1}{\tau}\int_{t_0}^{t} e^{s/\tau} T_{\text{ss}}(s)\,\mathrm{d}s\right]. \quad (7)$$

To carry out the validation, the instantaneous steady-state temperature was assumed to follow a sinusoidal variation: $T_{\text{ss}}(t) = A\sin\left(\frac{2\pi t}{L}\right) + C$, and the initial conditions were set to $T_{\text{trans}}(0) = T_{\text{ss}}(0) = C$. The interpretation is that a fast varying $T_{\text{ss}}(t)$ corresponds to fast changes in external conditions (such as irradiance). True external conditions time series could be Fourier-decomposed into multiple frequencies, which further motivates using sinusoidal functions as a validation set. This validation involves therefore three different timescales: the thermal relaxation time, the perturbation period and the discretisation timestep duration. Without loss of generality, the relaxation time τ was fixed and the two others varied.

The mean absolute error, normalised by the sinusoid amplitude A (nMAE), is then computed between the analytical average transient temperature, $\langle T_{\text{trans}}^{\text{analytic}}(t)\rangle_{dt}$ and the temperature computed with the PVsyst transient model, itself using the analytical average steady-state temperature, $\langle T_{\text{ss}}(t)\rangle_{dt}$ as input. Results are shown in Figure 1: the additional smoothing from equation (4) improves the model accuracy for all sinusoidal periods and all measurement time steps. Additionally, the increase of the cut-off time Δt_c beyond 20 min improves the model accuracy for longer time steps.

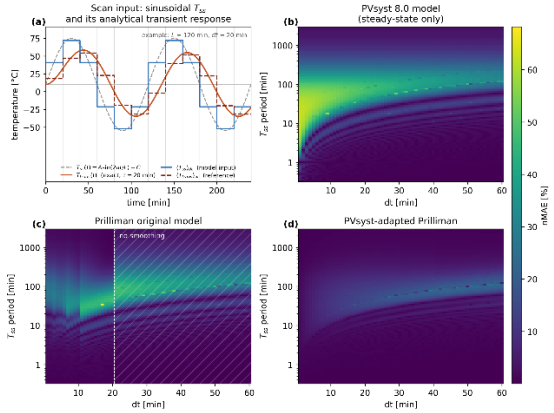


Figure 1: Results of the analytical model validation: (a): input sinusoidal steady-state temperature and corresponding analytical transient temperature. (b): discrepancy between steady-state and analytical transient temperatures. (c), (d): discrepancy between analytical and modelled transient temperatures for original Prilliman model and PVsyst adapted model.

3 TEMPERATURE MODEL VALIDATION

PVsyst's transient model is validated against 1-minute measurements from two arrays of the NIST campus [4]. Two fixed-tilt, south-facing installations are used to check for a potential bias related to the installation type:

- The ground array, an open-field, fixed-tilt (20°) installation of 271 kWp with c-Si modules.
- The roof array, a flat-roof installation (10° tilt) of 73 kWp using the same modules.

Both arrays are modelled in PVsyst 8.1 and simulated at a 1-minute time step over the year 2017, with the measured plane-of-array irradiance (POA), ambient temperature and wind speed as inputs.

3.1 Dataset and filtering

Both installations are studied using data from 2017. The POA is measured by a thermopile pyranometer for the ground array, and a class A silicon-cell pyranometer for the roof array. The silicon-cell sensor was preferred for its spectral response, but the equivalent device on the ground array could not be used because of calibration issues. Ambient temperature and wind speed were taken from array-level measurements. Each array carries several resistance temperature detectors (RTD) on the module backsheets, whose average is taken as the measured module temperature. Finally, the DC yield comparison of Section 4 uses the measured inverter DC power.

The 2017 dataset is filtered as follows: datalogger data quality flags are used to remove erroneous readings, and physically implausible measurements are also removed. Days with more than one hour of missing data are removed in full, as are eleven further days on the ground array affected by inverter clipping or faulty voltage readings. A

10.4229/EUPVSEC2026/4CV.1.3
020296-002

malfunction of the snow sensor was suspected, together with a possible discrepancy in snow depth between the weather station and the two array locations. The winter months, December to March, were therefore excluded altogether. Finally, only minutes with an irradiance above 10 W/m² and a sun elevation above 30° are retained, to exclude shading and building-model errors from the study.

3.2 Heat transfer coefficients

The PVsyst heat transfer coefficients U in equation (1) are effective parameters that should ideally be calibrated. A linear model is fitted when only irradiance and temperatures are available to compute a single U coefficient, or a bilinear model is fitted when a local wind measurement is available, yielding a set of two coefficients U_c and U_v. All three coefficients were fitted for each installation, covering the two situations a user can face. Additionally, simulations were carried out with the default U coefficient values recommended by PVsyst for each system type. Figure 2 shows an example of fit for the roof installation, while Table I summarises all U values used in this study.

Table I: Heat transfer coefficient values for the studied NIST PV arrays

	Ground	**Roof**
U (W_s=0)	32.16 [W/m²/K]	21.72[W/m²/K]
U_c	26.42 [W/m²/K]	19.77 [W/m²/K]
U_v	2.89 [Ws/m³/K]	1.23 [Ws/m³/K]
Default U	29 [W/m²/K]	20 [W/m²/K]

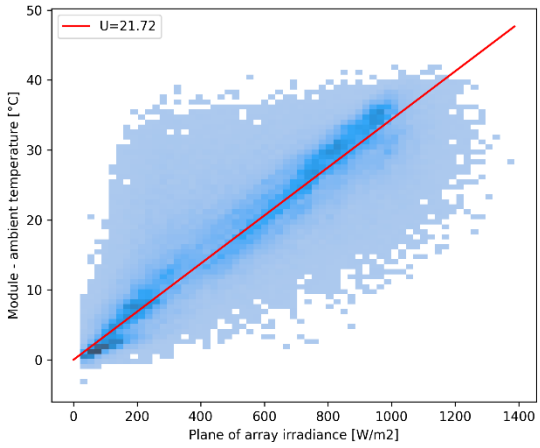


Figure 2: Example of fit for the roof installation in the no-wind case, U = 21.72 W/m²/K.

3.3 Modelled temperature precision

Module temperature was modelled over the eight retained months at the 1-minute scale, using both the steady-state and the transient models and each of the 2 sets of U coefficients. For each time step, the difference between simulation and measured value was computed. Results are shown in Figures 3 and 4 for both installations.

Table II summarises the mean bias error (MBE) and root mean square error (RMSE) observed for each scenario. For all sets of heat transfer coefficients, the transient model improves the temperature RMSE by about 2 °C but does not significantly affect the MBE. Using a set of two thermal coefficients to take the wind cooling effect into account further reduces the temperature RMSE. MBE is only affected by the calibration of the heat transfer coefficients. Using uncalibrated heat transfer coefficients results in a bias of 1–1.5 °C on average.

Table II: Error on modelled temperature for steady-state and transient models in all scenarios.

Model	**Ground**		**Roof**	
	MBE [°C]	**RMSE [°C]**	**MBE [°C]**	**RMSE [°C]**
U transient	0.12	2.66	-0.54	2.28
U steady state	0.22	3.91	-0.48	4.81
UcUv transient	0.00	1.64	-0.48	1.94
UcUv steady state	0.05	3.37	-0.41	4.74
Default transient	1.64	3.30	1.13	2.61

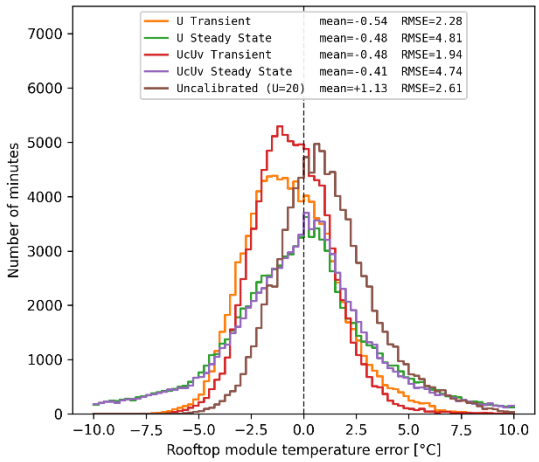


Figure 3: Error on module temperature models for the rooftop installation. Models show a slight temperature overestimation.

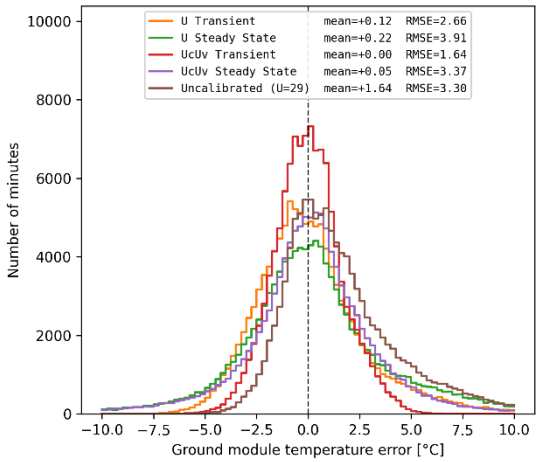


Figure 4: Error on module temperature models for the ground installation.

4 IMPACTS ON DC YIELD SIMULATION

The simulations of the NIST installations were also used to obtain the expected DC production of both arrays. In a first step, a reference simulation using the measured module temperature is compared to the different yield predictions based on temperature models. Then, the DC yield predictions are compared to the measured power. All

10.4229/EUPVSEC2026/4CV.1.3
020296-003

yields are normalised to the nominal power of each installation.

4.1 Reference simulation

The differences between the reference simulation and the simulations using temperature models are shown in Figure 5. The MBE and RMSE values are summarised in Table III. For all simulations, the MBE on DC production coming from the temperature model remains below 0.5 %. The trends observed at the temperature model level propagate to the DC yield modelling: the transient temperature model reduces the RMSE in all scenarios. Taking wind cooling into account further reduces the RMSE for the ground array but the effect is no longer significant for the rooftop installation. Finally, using uncalibrated heat transfer coefficients results in an expected MBE of 0.5 % on the DC yield.

Table III: Expected error on modelled DC yield.

Model	Ground		Roof	
	MBE [%]	RMSE [%]	MBE [%]	RMSE [%]
U transient	-0.02	0.90	0.18	0.77
U steady state	-0.18	1.19	-0.11	1.56
UcUv transient	0.02	0.54	0.17	0.63
UcUv steady state	-0.13	0.99	-0.13	1.55
Default transient	-0.51	1.14	-0.40	0.96

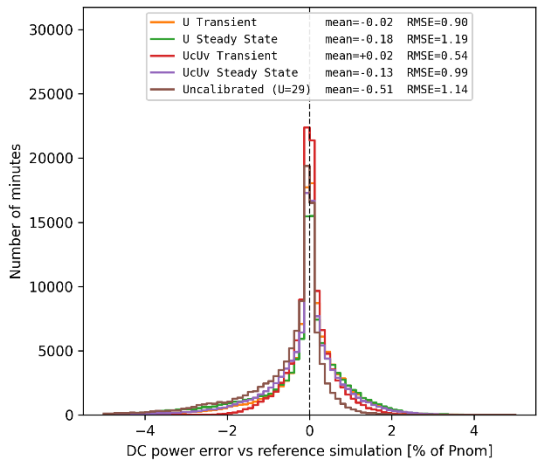


Figure 5: Roof installation: error on predicted DC yields between simulations, normalised to nominal power.

4.2 DC measurements

The different simulations were further compared with the inverter DC power measurements and results are presented in Table IV. The reference simulation using measured module temperature shows an MBE on DC production of −1.7 % for the ground installation, while being close to zero for the roof installation. This difference between installations is mainly attributed to the spectral responses of the POA sensors.

For both installations, the RMSE values are comparable for all thermal models studied (Figure 6), which shows that the error between simulated and measured DC yield is dominated by other sources. Concerning the MBE, only the use of uncalibrated heat transfer coefficients results in a visible difference (−0.4 %) compared with the reference simulation.

Table IV: Error on modelled DC yield compared to measured yield.

Model	Ground		Roof	
	MBE [%]	RMSE [%]	MBE [%]	RMSE [%]
Measured temp.	-1.77	4.99	-0.09	3.64
U transient	-1.79	5.07	0.10	3.72
U steady state	-1.95	4.89	-0.20	3.76
UcUv transient	-1.75	5.04	0.08	3.69
UcUv steady state	-1.90	4.86	-0.22	3.76
Default transient	-2.28	5.14	-0.49	3.72

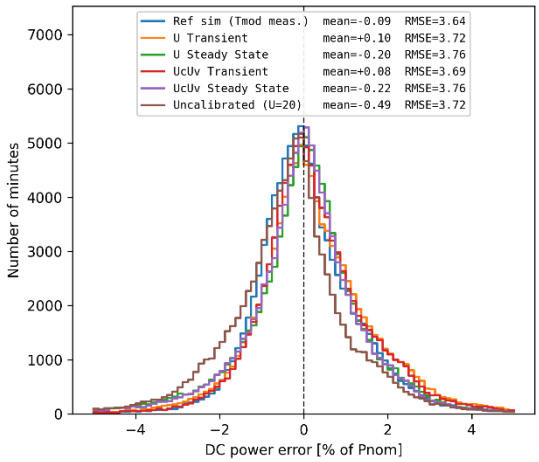


Figure 6: Roof installation: error between measured DC yields and simulated yields

4.3 Timestep cross-checks

A final cross-check was carried out to verify the impact of the simulation timestep on the accuracy of the temperature transient model using the roof array. Simulations were run with the U_c and U_v coefficient set, using the wind measurement, for time steps of 2, 5, 10 and 15 minutes.

The MBE and RMSE of modelled temperature TArray and DC power shows little to no sensitivity to the discretisation time step as shown in Table V. This shows that the model retains its accuracy and precision at different time steps.

Table V: Effect of the simulation time step on the transient model, using the wind measurement.

dt [min]	TArray vs meas.		DC power vs ref. sim.	
	MBE [°C]	RMSE [°C]	MBE [%]	RMSE [%]
1	-0.48	1.94	0.17	0.63
2	-0.51	1.96	0.19	0.64
5	-0.55	2.00	0.21	0.66
10	-0.58	2.01	0.21	0.66
15	-0.59	2.01	0.21	0.65

5 CONCLUSION

PVsyst's transient model clearly improves the modelling of PV array temperature over PVsyst's previous steady-state model by strongly reducing the temperature RMSE by 2 °C. It does so equally well for open and rooftop installations and can be applied at different discretisation time steps between 1 minute and 1 hour. Calibrating the heat transfer coefficients U for a given

10.4229/EUPVSEC2026/4CV.1.3
020296-004

system is an effective way to reduce the bias in modelled temperature. Where calibration is not possible, the default PVsyst U values remain a sound choice, leaving an expected bias of 0.4–0.5 % on DC energy yield in the examples studied. Finally, when a local wind measurement is available, using both the Uc and Uv thermal coefficients further reduces the RMSE of the temperature model.

6 REFERENCES

[1] M. Oliosi, B. Wittmer, A. Mermoud, A. Bridel-Bertomeu, and R. Vincent, "Implementation of a Sub-Hourly Clipping Correction in PVsyst," Proc. 41st European Photovoltaic Solar Energy Conf. & Exhib. (EU PVSEC), Vienna, Austria, 23–27 Sept. 2024. doi: 10.4229/EUPVSEC2024/4DV.4.7.

[2] S. E. Frid, A. V. Mordynskii and N. R. Avezova, "The Influence of a Photovoltaic Module Thermal Model Choice on the Error of Calculating the Module Performance," Applied Solar Energy, vol. 59, p. 480–487, August 2023.

[3] M. Prilliman, J. S. Stein, D. Riley and G. Tamizhmani, "Transient Weighted Moving-Average Model of Photovoltaic Module Back-Surface Temperature," IEEE Journal of Photovoltaics, vol. 10, p. 1053–1060, July 2020.

[4] L. Deville, M. Theristis, B. H. King, T. L. Chambers and J. S. Stein, "Open-source photovoltaic model pipeline validation against well-characterized system data," Progress in Photovoltaics: Research and Applications, vol. 32, p. 291–303, 2024.

[5] Boyd M, Chen T, Dougherty B “NIST Campus Photovoltaic (PV) Arrays and Weather Station Data Sets,” National Institute of Standards and Technology. U.S. Department of Commerce, Washington, D.C, 2017 [Data set].